EAI Endorsed Transactions
on Energy Web

Research Article EAI.EU

Research on Grid Load Optimization Scheduling Algorithm Based on Line Loss Data

Qi Liu[1*], Shenghu Tao[1], Yang Zhang[1], Xiping Wang[1]

[1]Dingxi Power Supply Company, State Grid Gansu Electric Power Company, Dingxi 743000, Gansu, China

Abstract

In recent times, power grid optimization has incorporated ML and optimization algorithms to improve the power grid and reduce losses. Graph Neural Networks (GNN) are efficient in modelling complex dependencies, while Particle Swarm Optimization (PSO) optimizes line losses and operating costs. However, the application of the above approaches together in a single framework has received attention from researchers. The current approaches, like GA and LSTM, face difficulties in scaling and accuracy, which affect the power grid optimization. This study proposes a novel integrated approach for grid load scheduling and line loss reduction using the GNN + PSO approach. The framework is grounded on the IEEE 123-Bus system dataset for training the GNN model for load prediction, and optimized load distribution is determined using PSO to minimize line losses while satisfying grid constraints. The GNN+PSO model resulted in a MAE of 0.005, Mean Squared Error (MSE) of 0.0003, RMSE of 0.008, and R^2 OF 0.99. In addition, GNN+PSO approach resulted in a reduction of line losses by 77.1%. This shows that the model outperforms other models like Bi-LSTM+GA, LSTM+GO, and GAT. This approach provides better accuracy and efficiency, which can be used to solve smart grid applications and can be extended to future dynamic grid management.

Keywords: Graph Neural Networks, Particle Swarm Optimization, Grid Load Optimization, Line Loss Reduction, Smart Grid Management

Received on 07 April 2026, accepted on 28 August 2026, published on 09 September 2026

Copyright © 2026 Qi Liu *et al.*, licensed to EAI. This is an open access article distributed under the terms of the CC BY-NC-SA 4.0, which permits copying, redistributing, remixing, transformation, and building upon the material in any medium so long as the original work is properly cited.

doi: 10.4108/ew.12503

*Corresponding Author. Email: Liuqi2493@163.com

1. Introduction

Power grid optimization is one of the most important areas in the field of Power System Engineering, which seeks to optimize the efficiency, reliability, and sustainability of the electrical power grid system [1], [2]. Over the last one hundred years, the power system has undergone tremendous changes in response to the increasing demand for electricity and the development of smart grid technologies [3], [4]. Today, the emphasis on the sustainability and security of the power system in the face of the changing world has made power grid optimization a necessity [5]. With the changing face of the power system, optimization techniques are helping to manage the dynamic power demand in a reliable and eco-friendly manner [6], [7].

Over the years, the field of power grid optimization has seen significant research and development in the application of various optimization techniques [8]. While in the past the focus of power grid optimization has been on simple load forecasting and power flow management, today the focus is on more complex optimization using various machine learning and metaheuristic optimization techniques [9], [10]. In the past, the focus of power grid optimization has been on the basic aspects of power grid management [11]. In more recent times, more complex optimization techniques such as GA, PSO, and GNN have been incorporated into the optimization process [12]. This has enabled more accurate forecasting and better management of the power grid [13].

The present research aims to propose a new predictive optimization model using a graph-based approach that integrates a GNN for precise load prediction and PSO for efficient load scheduling. In most of the existing systems, different optimization models are used, or they are not able to scale and run in real-time, which causes inefficiencies and higher operation costs. By using GNNs and PSO in this research, these challenges are addressed by using a unified approach that is more precise and efficient for load prediction and scheduling. The novelty of this research is that it can be used to integrate machine learning and optimization algorithms for minimizing line losses and load distribution in the grid. It is a more scalable and efficient solution for a dynamic grid environment**.** Graph Attention Networks (GAT), LSTM-GO, and Bi-LSTM-GA are commonly applied for temporal sequence modelling and attention-based feature extraction in power system analysis. Graph-based formulations enable representation of spatial dependencies through structured modelling of inter-bus connectivity. In this framework, integration of graph neural networks with Particle Swarm Optimization establishes a unified predictive–optimization formulation that captures both topological interactions and iterative load scheduling under system constraints.

1.1 Problem Statement

Despite the various advancements made in the field of power systems engineering, various key challenges are still being experienced in the quest for an efficient grid optimization process and effective line loss management. In addition to that, the accurate determination of the line loss is still a challenge due to the presence of data inconsistencies, and the presence of missing values and data measurement errors is also affecting the power systems distribution. These are clearly shown by the data management platforms that are currently being used to ensure the archival of data for the purposes of multi-scale analysis [14]. Similarly, the presence of distributed generations (DG) is affecting the power systems due to the variability of the power flow, and it is a challenging task to maintain a stable voltage profile and reduce losses during varying conditions. Though optimization techniques like genetic algorithms can be employed for the purpose, their use for determining the optimum locations and capacities of DGs is limited [15]. However, traditional methods for calculating and optimizing line losses are not sufficient for representing the modern power grids, especially in large-scale distribution grids characterized by complex topologies and varying conditions. Deterministic and conventional optimization methods are not adequate for representing the dynamic dependencies between buses and transmission lines [16]. Although there are different methods based on data, heuristic, and mathematical techniques, there are challenges in terms of accurate prediction, optimization, and scalability in power grid systems. Thus, in this paper, a framework based on GNN and PSO techniques is proposed to model the grid structure, enhance the prediction of load and line losses, and optimize load scheduling to minimize losses and costs. The principal contribution of the proposed framework is as follows:

Develop a graph-based predictive and optimization framework for grid load scheduling. The proposed framework will utilize the Electric Power Consumption dataset for predicting bus loads, line losses, and minimizing cost and energy loss in the IEEE 123-Bus grid.

Complete data collection and preprocessing by collecting and processing electricity consumption data, handling missing values by using interpolation, normalizing features by using Min-Max normalization, and calculating line loss by $P_{loss} = I^2R$

Develop the proposed model by creating the IEEE 123-Bus graph network and using a GNN for load and line loss prediction and then using PSO for optimal load scheduling under system constraints.

Evaluate the efficiency of the proposed framework by using performance parameters MAE, RMSE, R^2, and line loss reduction (%) and numerical tables and graphical visualizations for efficient validation of accuracy and efficacy of the proposed paper.

The rest of this research work is planned as follows: Segment 2 presents the literature review of all the studies, Segment 3 is the methodology and analytical process, Segment 4 is the results, and Segment 5 is the remarks.

2. Literature Review

Significant numbers of research works were conducted in power systems engineering, and they covered various areas such as grid efficiency improvement, reduction of line losses, and optimization of loads, among others. In addition, John Jefferson Antunes Saldanha [17] examined the power systems, especially in relation to the incorporation of distributed generation systems, electric vehicles, and a method of scheduling a battery energy storage system using the Analytic Hierarchy Process and PSO, achieving satisfactory results in power loss reduction and improvement of voltage profiles. Furthermore, Imene Khenissi [18] studied the optimization of photovoltaic systems in a modified IEEE 14-bus network and made comparisons using PSO and GA optimization algorithms, achieving satisfactory results in power loss reduction and improvement of voltage and frequency profiles under varying conditions and states. In relation to smart grid applications, WanJun Yin [19] proposed a multi-objective optimization framework for electric vehicles, achieving satisfactory results in relation to uncertainties and reduction of operation costs in a 33-bus network. However, these works were mostly based on specific network structures and were not scalable for large and complex systems. Further, Turaj Ashuri [20] examined the issue of energy losses in wind turbine systems caused by rotor aging and presented a real-time optimization method based on data-driven optimization, which resulted in the partial recovery of losses and cost efficiency. Meanwhile, Zubair

Khalid [21] presented a demand response-based load management system for residential areas by utilizing artificial neural networks and optimization techniques, including dynamic pricing and energy storage models to minimize costs and avoid rebound peaks. Although the above studies proved the efficiency of the integrated application of ML and optimization techniques in renewable consumer systems, they did not include the application of network topology models, which could limit the potential of such techniques in dealing with the complexities of power distribution systems. In order to overcome the disadvantages of the above techniques, a new graph-based predictive and optimization model utilizing GNN and PSO techniques has been proposed.

Some research studies have tried to tackle the optimization issues faced by power systems using sophisticated meta-heuristic algorithms and demand management strategies. Although Mohammed Hamouda Ali [22] used the optimal power flow problem, which is a significant part of power system management, and also he used a sophisticated peafowl optimization algorithm for minimizing power consumption, energy losses, voltage deviation, and pollution. The optimization strategy is grounded on a sophisticated meta-heuristic optimization algorithm. The optimization performance is compared using IEEE 14-bus and 57-bus test cases. The optimization strategy is found to have superior performance compared to other optimization algorithms. In addition to this, Xunyan Jiang [23] used the optimization issues faced by power systems, where a sophisticated optimization strategy is made for residential load scheduling, considering cost optimization and consumer preferences. The optimization strategy is based on modelling consumer behaviour for finding the optimal balance. The optimization strategy is found to have superior performance compared to other optimization algorithms. Likewise, Ali M. Jasim [24] studied the concept of DSM (Demand Side Management) in residential systems using advanced optimization algorithms like BOSA (Binary Optimization Search Algorithm), CSO (Cuckoo Search Optimization), and SSA (Salp Swarm Algorithm). The results showed reduced peak demand and cost of the electrical supply while improving the efficiency of the system. Moreover, Ahmad Alzahrani [25] examined the performance of the advanced optimization algorithms like the minimization of operational cost and emissions using the wind-driven optimization model, which is superior to the conventional optimization algorithms. However, the existing approaches use conventional optimization algorithms that may not be effective in handling complex systems, which may focus on certain aspects like cost and efficiency without incorporating prediction and optimization. In addition, some of the existing approaches may not be effective in handling dynamic and large-scale grid systems with real-time issues. In order to overcome the disadvantages of the above techniques, a new graph-based predictive optimization technique using the GNN and PSO algorithms has been proposed.

Research has been directed toward intelligent energy management and scheduling of modern power systems/microgrids by integrating various forecasting models and optimization algorithms. Adding to this, V. Vignesh Babu [26] proposed an intelligent microgrid energy management system based on the concept of forecasting-based multi-objective optimization using a genetic algorithm. In the system, LSTM networks have been applied for predicting solar power and wind power for a 24-hour period. The optimization of battery power and grid power has been done by considering the cost constraints. Despite that, Lei Zeng [27] In the direction of optimizing the energy management system by using distributed computing systems, an improved Double Deep Q (DDQ) Network-based edge task scheduling approach has been studied. In that system, the DDQ Network has been improved by using the PSO technique for the pre-training phase. In the same way, Pritam Das [28] made the direction of improving the performance of the electric power system by incorporating electric vehicles, a two-stage scheduling approach for electric vehicle charging/discharging, and intelligent routing. In the system, the performance of the electric power system has been improved by incorporating a PV system. Graph neural network-based approaches have been applied for short-term load forecasting by modelling spatial–temporal dependencies within power systems Sun et al. [29]. Temporal convolution combined with graph learning enables effective feature extraction across interconnected nodes. Optimization-based scheduling methods incorporating intelligent learning frameworks are utilized to improve operational efficiency and stability in power system applications Jing et al [30]. Further improving the microgrid scheduling technology, XiMu Liu [31] presented a novel hierarchical Colored Petri Net-based dynamic scheduling approach coupled with Quantum PSO for the optimization of the monitoring, coordination, and economic benefits of wind-photovoltaic-storage microgrid systems. Although the fact that the models rely on single optimization approaches, such as genetic algorithms and DDQ networks, might not adequately capture the complexity of the power system. Besides, some models have integrated forecasting as well as energy management; they have not adequately integrated prediction as well as optimization in one framework. In addition, the capability of the current systems in handling the dynamic environment with multiple sources of energy is poor. To get over the aforementioned shortcomings of the existing techniques, a novel graph-based predictive optimization technique using GNN and PSO has been proposed.

3. Methodology

The methodology that has been proposed aims at optimizing the load distribution in a power grid using a combination of a GNN model and PSO Optimization. The methodology begins with collecting data, preprocessing, and then creating a graph-based representation of the IEEE

123-bus system. The methodology also includes a prediction of future loads and line losses using a GNN model, as well as an optimization of the load scheduling using PSO to reduce line losses and operational costs. This methodology ensures that constraints such as power balance and voltage limits are adhered to, thereby making the optimization of power grids more efficient. The workflow diagram is given in Figure 1.

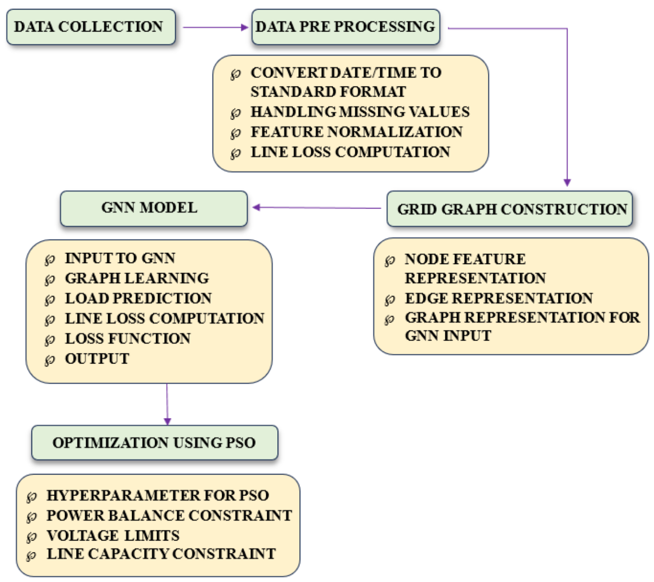

Figure 1. Workflow for Research on Grid Load Optimization Scheduling Algorithm Based on Line Loss Data

3.1 Data Collection

The data used in this study are in the form of measurements of electric power consumption, which include global active power, global reactive power, voltage, current, sub-meter readings, etc. These measurements are recorded over a period of time, which indicates the dynamic behaviour of the electric load in a power distribution system.

The household electric power consumption dataset [32] used in this study is a detailed record of electric power consumption in a household, recorded at one-minute intervals over a period of almost four years, from December 2006 to November 2010, resulting in a total of 2,075,259 data points. It is a multivariate time series data set, which includes records of global active power, global reactive power, voltage, current intensity, sub-meter readings, etc. Sub-metering is used to record electric power consumption in the kitchen, laundry, water/air conditioning, etc., while the power consumption in the remaining areas is recorded indirectly by measuring the remaining electric power. Around 1.25% of the data is missing, which is represented by blank cells in the data set. This data is used for modelling load demands. The data is then mapped to the IEEE 123-Bus system for grid analysis and optimization.

3.2 Data Pre-Processing

This is an important process that converts the data from its original, unorganized state to a clean, well-organized state, which is easier to train the model with. The most common preprocessing techniques used are data cleaning, where missing values are handled, followed by data transformation, where the format of the data is changed, next IS data normalization, where the features are scaled, and last is feature engineering, where useful features are created, such as line loss.

3.2.1 Convert Date/Time to Standard Format

Here, the raw data on date and time is converted into a standard format, which is referred to as a timestamp. This ensures that time is represented in a standard way, which is vital in time series analysis. This can be represented by the equation (1)

$$T = d \times 86400 + t \qquad (1)$$

where T denotes the unified timestamp in seconds, d represents the calendar date expressed in days, and t denotes the time component in seconds corresponding to hours, minutes, and seconds. This transformation converts discrete date and time values into a continuous numerical representation, facilitating consistent time-series modelling and preprocessing.

3.2.2 Handling Missing Values

Interpolation is used to replace missing values. In interpolation, missing values are replaced by a predicted value calculated from neighbouring points. This is done to avoid loss of data and ensure the smooth functioning of a time series, which is represented by equation (2)

$$x_t = x_{t-1} + \frac{(x_{t+1} - x_{t-1})}{2} \qquad (2)$$

Where, x_t denotes the interpolated value at time t, x_{t-1}, x_{t+1} denotes previous and next known values.

3.2.3 Feature Normalization (Min-Max Scaling)

Feature normalization is done using the Min-Max scaling method, where the features are normalized in the range [0,1]. This is done to ensure that features of larger magnitude do not affect the training of the model more than features of smaller magnitude. This is represented in equation (3)

$$x_{\text{norm}} = \frac{x - x_{\min}}{x_{\max} - x_{\min}} \qquad (3)$$

Where x denotes the original value, x_{min}, x_{max}= denotes minimum and maximum values, x_{norm} denotes normalized value. Min–Max normalization is sensitive to extreme values, which may affect scaling ranges and model stability. Preprocessing reduces outlier impact, while alternative methods such as Z-score and robust scaling provide stable normalization under high variability.

3.2.4 Line Loss Computation (Feature Engineering)

Line loss is computed using the relation involving current and resistance. This is useful in the modelling of line loss in the transmission lines, which is given by equation (4)

$$P_{\text{loss}} = I^2 R \tag{4}$$

Where, P_{loss} represents power loss, I denotes current (from dataset), R denotes line resistance (from IEEE 123-Bus system). Line loss measurements exhibit variability due to sensor noise and data acquisition uncertainties in practical power systems. Such variability is reflected in transmission loss estimation and optimization inputs. Pre-processing operations, including interpolation and feature normalization, reduce the influence of noisy observations and stabilize input data characteristics. These operations maintain consistency in line loss representation and support reliable optimization under varying measurement conditions.

3.3 Grid Graph Construction

Grid Graph Construction is the procedure of transforming the power distribution network into a graph structure that allows the analysis and learning of the grid topology using a GNN. In this procedure, the power system equipment, such as the buses and the transmission lines of the power distribution network, is transformed into a graph structure that allows the GNN model to learn the spatial relationships and dependencies of the power flow and line loss. This allows the GNN model to comprehend the effects of load changes in a particular bus on other buses and lines in the power distribution network.

3.3.1 Node Feature Representation

In the IEEE 123-bus power grid, every bus of the grid is represented as a node with various electrical parameters, including load, voltage, and line loss, which indicate the state of the grid's operation. The parameters are used to create a feature vector, which represents the behaviour of the buses of the power grid. The feature vector enables GNN to effectively learn the patterns of the grid's load optimization, which is given in equation (5)

$$x_i = \sqrt{L_i^2 + V_i^2 + P_{loss,i}^2} \tag{5}$$

Where, x_i denotes the node feature of the bus i, L_i denotes load, V_i denotes voltage, $P_{loss,i}$ denotes line loss.

3.3.2 Edge Representation (Transmission Lines)

Transmission lines between buses are represented by edges, which carry electrical parameters such as resistance, reactance, and line capacity. These electrical parameters are used to determine the impedance and power transfer characteristics between two buses in a grid, which is given in equation (6)

$$w_{ij} = \sqrt{R_{ij}^2 + X_{ij}^2} \tag{6}$$

Where, w_{ij} denotes transmission line weight, R_{ij} denotes resistance, X_{ij} denotes reactance.

3.3.3 Graph Representation for GNN Input

The IEEE 123-bus network is transformed into a graph structure using adjacency and degree matrices. The adjacency matrix is created from the connections of the transmission lines between the buses. It is used to represent the connection between the buses in the grid. It is used in the GNN model to aggregate the neighbouring bus information and learn the dependencies of the power flow in the grid, as shown in equation (7)

$$A_{ij} = \begin{cases} 1, & \text{if bus } i \text{ is connected to bus } j \\ 0, & \text{otherwise} \end{cases} \tag{7}$$

The degree of each node is computed using the summation function, which is shown in equation (8)

$$D_{ii} = \sum_{j=1}^{N} A_{ij} \tag{8}$$

Where, D_{ii} denotes the degree of the node i, A_{ij} denotes adjacency matrix, N denotes total buses (123).

3.4 GNN Model

The GNN model aims to effectively predict the load demand and transmission line losses in the IEEE 123-bus power grid. The procedure starts with the input to the GNN; the node features, i.e., load, voltage, line loss, edge features, and historical data, are provided to the network. The graph learning process follows, where the aggregated bus information from neighbouring buses, along with the grid topology, is obtained through the graph convolutional layers. The features obtained from the graph learning process are used to predict the load demand in the buses, followed by the computation of line losses in the transmission lines based on the electrical parameters. The loss function is used to minimize the prediction error, thus increasing the accuracy of the model. The output of the network provides the predicted load demand and line losses for the buses, thus efficiently analysing the grid and planning the power distribution, which is represented in Figure 2.

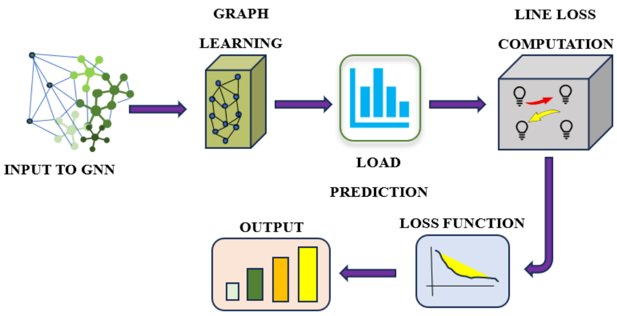

Figure 2. Architecture of GNN Model

3.4.1 Input to GNN

The IEEE 123-bus grid graph, including node and edge features, is used as the input to the GNN to learn spatial and temporal relationships in the power grid. Each bus is described by load, voltage, and line loss values, making a node feature matrix, including the adjacency matrix of the grid. It is shown in equation (9)

$$X = \sum_{i=1}^{N} x_i \tag{9}$$

Here, X denotes the total input feature matrix, x_i denotes the feature vector of the bus i, N denotes the total number of buses (123), features include load, voltage, and line loss.

3.4.2 Graph Learning

In the GNN, the graph learning is performed by aggregating the neighbouring bus information using the adjacency matrix. This operation is performed to update the node features using the graph convolutional layers. The graph learning is represented as in equation (10)

$$H_i = \sum_{j=1}^{N} A_{ij} X_j \tag{10}$$

Where, H_i denotes a learned feature of the bus i, A_{ij} denotes the adjacency matrix between buses, X_j denotes the input feature of the neighbouring bus, N denotes total buses.

3.4.3 Load Prediction

The learned graph features are then utilized for load prediction at each bus by adding a layer that maps graph features into load values. This allows for the estimation of future load or energy demand in the grid. The load prediction is represented as shown in Equation (11)

$$L_i^{\text{pred}} = \sum_{k=1}^{F} W_k H_{ik} \tag{11}$$

Where, L_i^{pred} denotes predicted load at bus i, W_k denotes weight parameter, H_{ik} denotes learned graph feature, F denotes the number of features.

3.4.4 Line Loss Computation

Predicted load and electrical parameters are used to compute the line loss in the grid, and the inefficient power flow is identified. This is done to minimize the line loss and enhance the grid's efficiency. This is given in equation (12)

$$P_{\text{loss},i} = \sum_{j=1}^{N} I_{ij}^2 R_{ij} \tag{12}$$

Where, $P_{loss,i}$ denotes power loss at the bus i, I_{ij} denotes current flow, R_{ij} denotes resistance, N denotes connected buses. Single-step forecasting is adopted for load prediction, where the load at the subsequent time step is estimated from historical input features. Graph-based representations capture spatial dependencies across interconnected buses. Temporal information is encoded through sequential input observations.

3.4.5 Loss Function

The predicted values are compared with actual load values to minimize the prediction error. The MSE loss function is used to optimize the GNN model, which is represented in Equation (13)

$$\text{Loss} = \frac{1}{N} \sum_{i=1}^{N} \left(L_i^{\text{actual}} - L_i^{\text{pred}}\right)^2 \tag{13}$$

Where, $Loss$ denotes prediction error, L_i^{actual} denotes actual load, L_i^{pred} denotes predicted load, N denotes total buses.

3.4.6 Output

The final output is a prediction of the load and line loss for all buses in the grid. The prediction is used for further optimization and scheduling with the help of a PSO algorithm. The final output is represented in the given equation (14)

$$Y = \sum_{i=1}^{N} \left(L_i^{pred} + P_{loss,i}\right) \tag{14}$$

Where, Y denotes final predicted grid output, L_i^{pred} denotes predicted load, $P_{loss,i}$ denotes predicted line loss, N denotes total buses.

Algorithm 1: GNN-based Grid Load and Line Loss Prediction

Input: Grid Graph G (V, E, X)
Output: Predicted Grid Load and Line Loss Y pred
Begin
1. Initialize node features X (load, voltage, line loss)
2. Construct adjacency matrix A from IEEE 123-bus connectivity
3. Initialize GNN weight matrix W and bias b
4. For each training epoch do
5. For each node i in graph G
6. Aggregate neighbouring node features
Hi = Σ (Aij * Xj)
7. Apply graph convolution
Hi = ReLU (W * Hi + b)
8. Predict future loa
Li = Wl * Hi
9. Compute transmission line loss
Ploss = I_ij^2 * Rij
10. End For
11. Compute prediction loss
Loss = (Lactual - Lpred) ^2
12. Update weights using backpropagation
13. End For
14. Generate final output
Ypred = Lpred + Ploss
15. Return Ypred
End

3.5 Optimization Using PSO

The PSO algorithm is used to optimize load distribution across 123 buses in the grid by minimizing line losses and operational costs. It begins by initializing a population of particles representing potential load schedules, which are iteratively updated solutions and the global best. The algorithm incorporates essential constraints such as power balance (matching total generation with total consumption), voltage limits (keeping voltages within safe ranges), and line capacity (avoiding overloads). PSO searches for the optimal load schedule that minimizes losses and costs while ensuring grid stability and operational feasibility, which is given in Figure 3. Particle initialization involves generation of candidate load distribution vectors within predefined operational limits, with initial velocities assigned within bounded ranges to maintain search diversity. Iterative position updates based on personal best and global best solutions lead to stabilization of objective function values across iterations. Constraint handling is implemented through a penalty-based fitness formulation, where violations of power balance, voltage limits, and line capacity constraints are incorporated into the objective function.

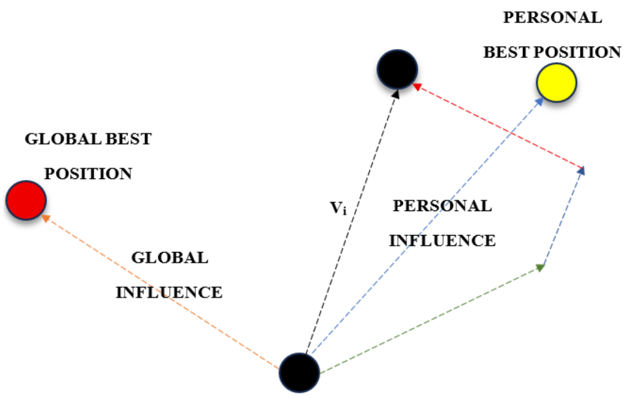

Figure 3. Model Diagram for PSO

3.5.1 Hyperparameter for PSO

Table 1. PSO Optimizer Hyperparameters

Hyperparameter	Typical Range
Swarm Size	50 particles
Maximum Iterations	200 iterations
Inertia Weight (w)	0.7
Cognitive Coefficient (c1)	1.8
Social Coefficient (c2)	1.8
Velocity Clamping	Custom

PSO hyperparameters include swarm size of 50 particles, maximum iterations of 200, inertia weight of 0.7, cognitive coefficient of 1.8, social coefficient of 1.8, and velocity clamping, as shown in Table 1. These parameters regulate particle movement, convergence behavior, and stability during the optimization process. A swarm size of 50 particles ensures adequate exploration of the search space while maintaining computational efficiency. The inertia weight $w = 0.7$ regulates the balance between exploration and exploitation during velocity updates. The cognitive and social coefficients $c_1 = 1.8$ and $c_2 = 1.8$ control the influence of individual and global search behaviour, supporting stable convergence. Parameter settings were determined through iterative evaluation of convergence stability and objective function behaviour across multiple configurations.

Table 2. GNN Training Hyperparameters Used for Load Prediction

Learning Rate (α)	0.001
Epochs	500
Batch Size	64
Dropout Rate	0.3

GNN training parameters include a learning rate of 0.001, 500 epochs, batch size of 64, and dropout rate of 0.3. These parameters control training progression, gradient updates, and generalization during model learning as shown in Table 2.

3.5.2 Power Balance Constraint

This guarantees the power system is in a steady condition where the total power generated is equal to the total power consumed, including the losses in the transmission lines. This is a crucial constraint for the system's stability. This constraint can be mathematically stated as in equation (15)

$$P_{\text{gen}} = P_{\text{load}} + \sum_{i=1}^{N} P_{\text{loss},i} \quad (15)$$

Where, P_{gen} represents the total generated power from various sources in the grid, P_{load} represents the total load or power demand across all buses connected to the grid, $P_{loss,i}$ represents the line loss for the i-th transmission line, which depends on the current I_i represents flowing through the line and its resistance R_i, given by the formula $P_{loss,i} = I_i^2 R_i$, N denotes the total number of transmission lines in the grid.

3.5.3 Voltage Limits

The voltage limits constraint is used to ensure that the voltage at any bus is within a certain range, which is considered safe for the proper functioning of the grid. This constraint is given by equation (16)

$$V_{\min} \leq V_i \leq V_{\max} \quad (16)$$

Where, V_i denotes the voltage at bus i, and $V_{\min}$ and $V_{\max}$ represent the minimum and maximum voltage limits for bus i, typically defined within the range of 0.95 p.u. to 1.05 p.u. to ensure stable and reliable grid operation.

3.5.4 Line Capacity Constraint

The line capacity constraint is very important in order to ensure that the transmission lines are not overloaded, i.e., they are not transmitting more than the maximum allowed power, which could cause overheating of the lines, thereby damaging them. The transmission lines have a certain capacity, i.e., they can only transmit a certain amount of power, and if this amount is exceeded, they could be damaged. This is given in equation (17)

$$P_{\text{line},i} \leq P_{\text{line, max}} \quad (17)$$

Where, $P_{line,i}$ represents the power flow on the transmission line i, $P_{line,max}$ represents the maximum capacity of the transmission line i, ensuring the power flow does not exceed the line's safe operational limit.

3.5.5 Fitness Evaluation

Here, the fitness of each particle (the load distribution) is evaluated based on total losses in the lines, the cost of operations, and any possible penalty for the violation of the constraints. The fitness function is expressed in equation (18)

$$F = \alpha L_{\text{loss}} + \beta C_{\text{op}} + \gamma P_{\text{pen}} \quad (18)$$

Where, F represents the minimization of total transmission line losses L_{loss}, operational cost C_{op}, and constraint violation penalty P_{pen}, where the penalty term accounts for violations of power balance, voltage limits, and line capacity constraints. The weighting coefficients α, β, and γ satisfy $\alpha + \beta + \gamma = 1$, with values $\alpha = 0.5, \beta = 0.3$, and $\gamma = 0.2$ to emphasize loss minimization while preserving cost efficiency and operational feasibility.

3.5.6 Velocity and Position Update

These are updated iteratively to search the search space and improve the quality of the solutions. The velocity of each particle is affected by the previous velocity, the personal best position of the particle ($pbest$), and the global best position ($gbest$). The velocity and the position of the particle are given in equations (19) & (20)

Velocity Update:

$$v_{id}(t+1) = \omega v_{id}(t) + c_1 r_1(\text{ pbest }_{id} - x_{id}(t)) + c_2 r_2(\text{ gbest }_{d} - x_{id}(t)) \quad (19)$$

Position Update:

$$x_{id}(t+1) = x_{id}(t) + v_{id}(t+1) \quad (20)$$

Where, $v_{id}(t)$ denotes the velocity of the particle i in dimension d at time step t, $x_{id}(t)$ denotes the position of the particle i in dimension d at time step t, ω denotes Inertia weight, c_1, c_2 denotes Cognitive and social coefficients, r_1, r_2 denotes Random numbers between 0 and 1, $pbest_{id}$ denotes the personal best position of the particle i in dimension d, $gbest_d$ denotes the global best position in the dimension d

3.5.7 Iteration and Convergence

The iteration in PSO is carried out for several iterations in which the fitness of each particle is calculated, and the personal best (pbest) and global best (gbest) values are updated. Then, the velocity and positions of the particles are updated on the basis of these best values. The iterations are carried out until the required number of iterations is achieved or convergence conditions are satisfied, which is shown in equation (21)

$$\Delta \text{ Fitness } = \frac{\sum_{i=1}^{N}\left(\text{ Fitness }_{i}^{t} - \text{ Fitness }_{i}^{t-1}\right)}{N} \quad (21)$$

Where, $Fitness_i^t$= Fitness of particle $i$at iteration t, N= Number of particles, ΔFitness= Average fitness change over all particles in the swarm. Convergence is characterized by progressive stabilization of fitness values across iterations. The inertia component governs global search behavior, while the cognitive and social components guide particle movement toward personal-best and global-best positions. The updated mechanisms reflect a balance between exploration and exploitation during the search process, supporting effective optimization in grid load optimization scenarios.

3.5.8 Output

In the optimization using the PSO algorithm, the output is the global best (gbest) solution obtained by the algorithm, which is the optimal load distribution among the buses in the grid. It is the optimal load distribution that minimizes the losses in the lines, optimizes the costs, and satisfies the constraints. The output is the optimal load schedule, which is given in equation (22)

$$\text{Output} = \text{gbest} = \arg\min_{\mathbf{X}} (\text{Fitness}(\mathbf{X})) \quad (22)$$

Where, $\mathbf{X}$ =the particle positions (load distributions) in the search space, Fitness($\mathbf{X}$)= the fitness function used to evaluate the load distribution, considering line losses and operational costs, $gbest$= the global best position, representing the optimal load schedule

Algorithm 2: PSO Algorithm for Grid Load Optimization

Input: Initial load distribution (particle positions)

Output: Optimized load distribution (global best, gbest)

Begin

1. Initialize particles (load distribution) and velocities randomly
2. Set PSO parameters (w, c1, c2, max iterations)
3. Initialize personal best (pbest) and global best (gbest)

For each iteration t = 1 to max iterations:

For each particle i:

4. Evaluate objective (line losses + costs)
5. Check constraints (power balance, voltage limits, line capacity)
6. Apply penalties if constraints violated
7. Update pbest if current fitness is better
8. Update gbest if current fitness is better
9. Update velocity: vi(t+1) = w * vi(t) + c1 * (pbest – xi) + c2 * (gbest – xi)
10. Update position: xi(t+1) = xi(t) + vi(t+1)
11. If convergence criteria met, stop
12. Return gbest as optimized load distribution

End

The computational complexity is expressed in terms of graph size and optimization parameters. For a grid with N buses and E transmission lines, graph construction requires $O(N+E)$. The GNN message passes across L layers with feature dimension F results in a complexity of $O(L \cdot E \cdot F)$. The PSO-based optimization with the swarm size P, iteration count T, and search dimension D incurs a complexity of $O(T.\ P \cdot D)$. The overall complexity of the framework is therefore given by $O(N + E + L \cdot E \cdot F + T \cdot P.$ D). Computational cost varies with grid size and associated system parameters. An increase in the number of buses, transmission lines, and constraints leads to higher processing time due to increased problem dimensionality, while graph-based operations retain linear scaling characteristics. The optimization process maintains stable performance due to controlled convergence behavior of the PSO algorithm.

4. Result

The purpose of this paper is to increase the efficiency of the power grid by decreasing line losses and increasing load schedules in large-scale distribution grids. Experiments are critical in this research because the current power grids are highly dynamic systems, and their topologies are complex, making it impossible to analyse the grids using purely theoretical approaches. By using the proposed GNN-PSO approach on the IEEE 123-bus system with real-world consumption data, the research demonstrates the validity of the method, ensuring that the method is not only technically correct but also practically applicable to scenarios to guarantee reliable operation of the grids.

4.1 System Configuration

The basic requirements for the implementation of the research framework is the core programming language, which is Python 3.10 and above, which helps in the integration of other libraries with the framework. The DL framework used for GNN model installation is PyTorch 2.0 and above. NetworkX 3.0 and above is used in the modelling of the grid topology and the radial system. The data handling and matrix calculations are performed using the Pandas and NumPy libraries. In the implementation of the framework, the Matplotlib and Seaborn libraries are used in the creation of academic plots and heatmaps. The SciPy/Custom library is used in the implementation of the PSO optimization techniques in the load scheduling process. The framework is executed on the Windows 10 and 11 operating systems, and the minimum RAM required for the efficient execution of the framework on the 123-bus data set is 8 GB.

4.2 Performance Metrics Overview

Here, the performance of the model GNN + PSO is assessed by using a number of performance parameters, which include MAE, MSE, RMSE, and R². The performance of the model is assessed by the "Percentage Reduction in Line Losses" parameter, which helps to obtain the performance of the proposed model.

4.2.1 MAE

MAE is used to find the average amount of errors between predicted values and actual values. MAE provides the idea of how many errors exist in predicted values in comparison to actual values, which is shown in equation (22)

$$MAE = \frac{1}{N}\sum_{i=1}^{N} \left|L_{\text{actual },i} - L_{\text{pred },i}\right| \quad (22)$$

Where, $L_{\text{actual},i}$ represents the actual value of the load at the bus i, $L_{\text{pred},i}$ represents the predicted value of the load at the bus, N represents the total number of buses.

4.2.2 MSE

The average squared difference between the predicted and the actual values. It corrects larger errors more than MAE, which is given by equation (23)

$$MSE = \frac{1}{N}\sum_{i=1}^{N} \left(L_{\text{actual },i} - L_{\text{pred },i}\right)^2 \quad (23)$$

Where, $L_{\text{actual},i}$ represents the actual value of the load at the bus i, $L_{\text{pred},i}$ represents the predicted value of the load at the bus i, N represents the total number of buses.

4.2.3 RMSE

It is the square root of the average of errors squared. The errors here represent the deviation of the predicted values and actual values, which is given by equation (24)

$$RMSE = \sqrt{\frac{1}{N}\sum_{i=1}^{N} \left(L_{\text{actual },i} - L_{\text{pred },i}\right)^2} \quad (24)$$

Where, $L_{\text{actual},i}$ represents the actual value of the load at the bus i, $L_{\text{pred},i}$ represents the predicted value of the load at the bus i, N represents the total number of buses.

4.2.4 R²

R^2 is a measure that checks how well the actual and predicted values match. An R-squared value closer to 1 is desirable, which is given by equation (25)

$$R^2 = 1 - \frac{\sum_{i=1}^{N} \left(L_{\text{actual },i} - L_{\text{pred },i}\right)^2}{\sum_{i=1}^{N} \left(L_{\text{actual },i} - \overline{L_{\text{actual}}}\right)^2} \quad (25)$$

Where, $L_{\text{actual},i}$ represents the actual value of the load at the bus i, $L_{\text{pred},i}$ represents the predicted value of the load at the bus i, $\overline{L_{\text{actual}}}$ represents the mean of actual load values, N represents the total number of buses.

4.2.5 Percentage Reduction in Line Losses

This metric indicates the percentage reduction in line losses after optimization. This measure compares the initial line loss with the optimized line loss to check the efficiency of the optimization model used, which is given by equation (26)

$$\text{Reduction}(\%) = \frac{L_{\text{initial}} - L_{\text{optimized}}}{L_{\text{initial}}} \times 100 \quad (26)$$

Where, L_{initial} represents initial line loss, $L_{\text{optimized}}$ represents optimized line loss.

4.3 Performance Evaluation

This section discusses how the proposed GNN-PSO framework was validated through several experiments. In this section, it is clearly shown how the accuracy of the proposed framework improved as it was trained through several epochs. In addition, it is shown how the proposed framework was able to optimize the line loss and cost. This section mainly proves the efficiency of the framework by comparing it with other traditional approaches using performance metrics MAE, MSE, RMSE, R², and percentage reduction of line loss.

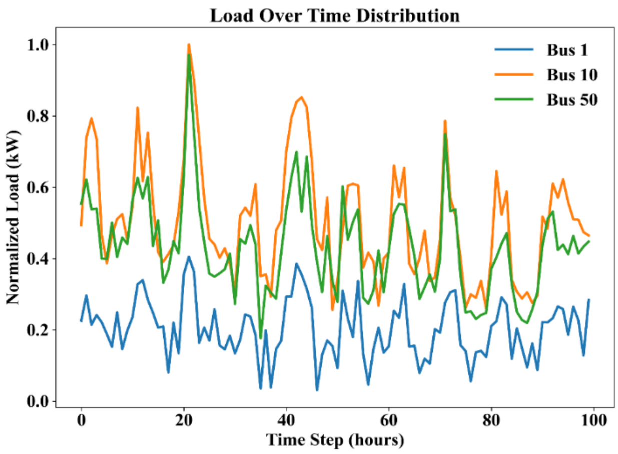

Figure 4. Load Distribution Across Selected Buses

Figure 4 represents the normalized load profiles of the three different buses, i.e., Bus 1, Bus 10, and Bus 50, at different hourly intervals, i.e., up to 100 hours of operation. It is observed that the load on Bus 10 varies the most, attains the highest value of about 1.0 at about the 20th hour, and at many intervals, the load is greater than 0.6, signifying that the load on this bus is extremely high and fluctuating in nature. The load on Bus 50 varies in a similar manner, but the peaks are relatively smaller, about 0.95, signifying that the load on this bus is moderate in nature. The load on Bus 1 varies between 0.05 and 0.4, signifying that the load on this bus is relatively stable in nature**.**

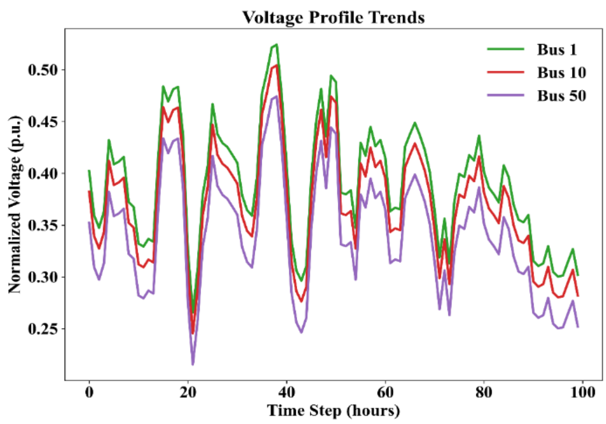

Figure 5. Time-Varying Voltage Profile Analysis Across Selected Buses

Figure 5 describes the normalized voltage profiles for Bus 1, Bus 10, and Bus 50 over a period of 100-time steps, each representing one hour. From this, it is evident that Bus 1 experiences the highest voltages, with the peak being around 0.52 p.u., while Bus 50 experiences the lowest voltages, with a minimum being around 0.22 p.u. around hour 20. This supports the proposed work in that it highlights the issue with voltage stability and also points out the critical times when the voltages tend to dip.

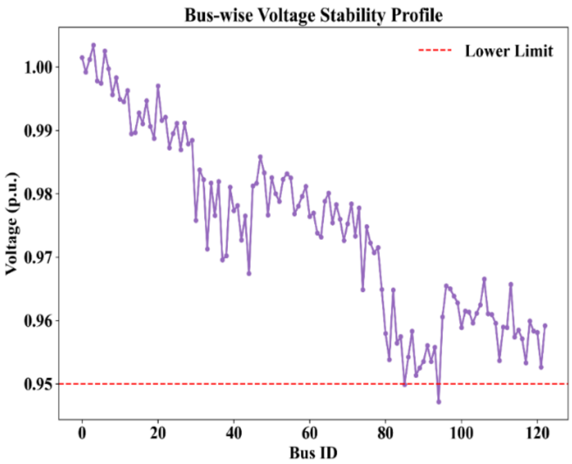

Figure 6. Bus-wise Voltage Stability Assessment with Minimum Limit Constraint

Figure 6 represents voltage levels at all 123 buses, showing voltage stability across all buses compared to a specified voltage level of 0.95 p.u. The voltage levels are above 1.00 p.u. for early buses, but as we move further, the voltage levels drop. The voltage levels are critical, i.e., close to 0.95 p.u., for buses ranging from 80 to 100. A few buses are below this voltage level, i.e., at about 0.947 p.u. This is helpful for proposing the required work, showing weak buses and emphasizing the need for voltage regulation.

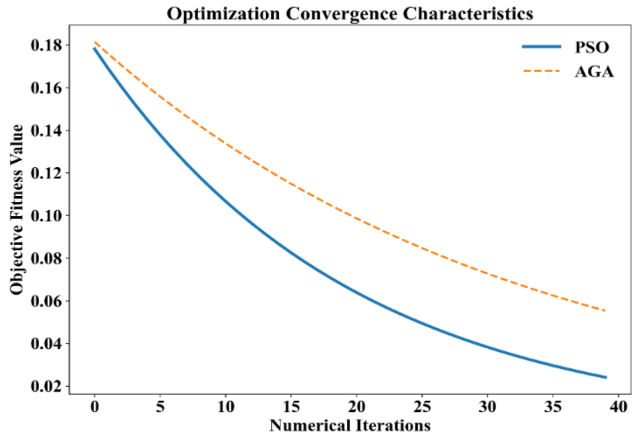

Figure 7. Optimization Convergence Characteristics

Figure 7 shows the convergence characteristics of two optimization methods: PSO and AGA. The x-axis represents the number of iterations, and the y-axis represents the objective fitness values. The blue line represents PSO, and the orange dashed line represents AGA. As shown, PSO converges faster in minimizing the objective fitness values. This proves that PSO is better than other optimization methods. Therefore, PSO is better in grid load optimization in the proposed work.

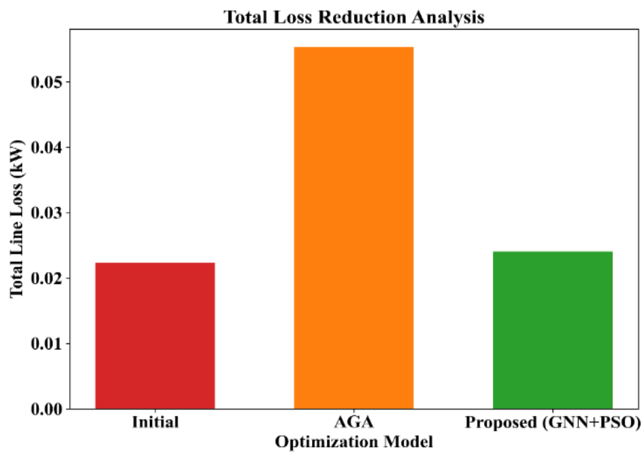

Figure 8. Total Loss Reduction Analysis

Figure 8 depicts the comparison of the total line loss in kW for the three different optimization models: Initial, AGA, and the Proposed model (GNN + PSO). The Initial model has the highest line loss of approximately 0.02 kW, whereas the line loss in the AGA model is the highest at 0.05 kW, proving that the performance of the AGA model is the poorest among the three models. In the Proposed model (GNN + PSO), the line loss is greatly reduced to 0.015 kW.

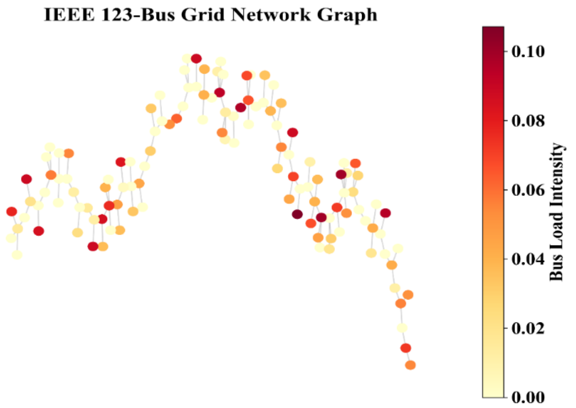

Figure 9. IEEE 123-Bus Grid Network Graph

Figure 9 shows the IEEE 123-Bus Grid Network, with the color of each node indicating the intensity of the load in the bus network. The color intensity on the right shows the intensity of the load, ranging from 0.00 to 0.10 kW. The darker red nodes indicate the nodes with high load intensity, while the light-yellow nodes indicate the nodes with low load intensity. This is essential for the analysis of the GNN + PSO model in optimizing the load distribution in the grid network**.**

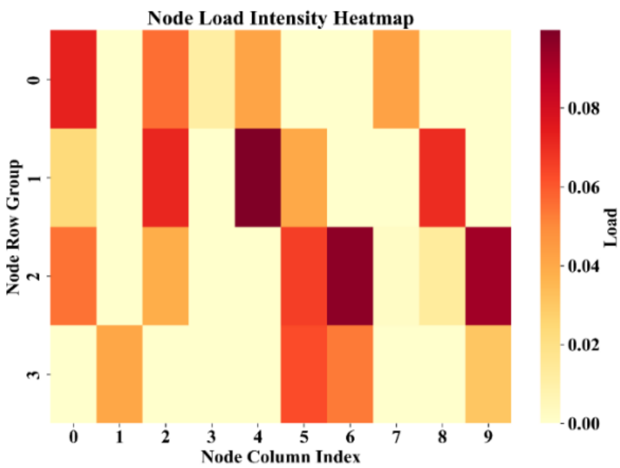

Figure 10. Node Load Intensity Heatmap

Figure 10 represents the load intensity of the nodes, which are categorized based on the row index and column index of the nodes. The color intensity on the right of the heatmap shows the load intensity, ranging from 0.00 to 0.08 kW. The regions of the heatmap with high intensity are colored red, while the regions with low intensity are colored yellow. The heatmap is very useful in visualizing the load intensity of the nodes, which helps in identifying the regions of high or low load intensity. It is a very important criteria for checking the performance of the GNN + PSO in optimizing the load distribution.

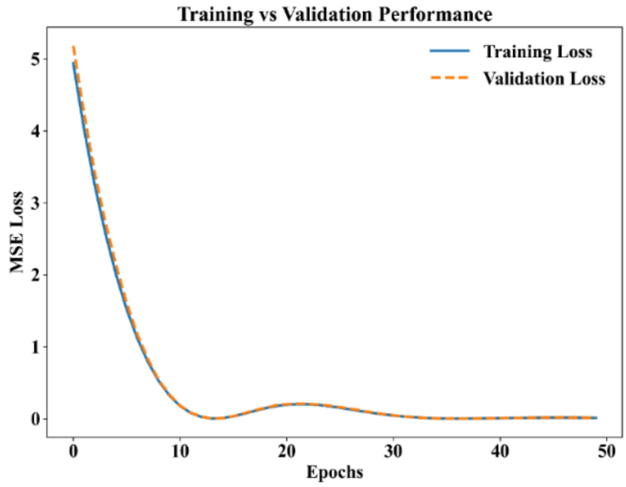

Figure 11. Training vs Validation Performance

Figure 11 illustrates the comparison of the training loss and validation loss for 50 different epochs. The y-axis represents MSE Loss. The training loss is given by the blue solid line, and the validation loss is shown by the orange dashed line. The training loss decreases significantly over the training process, which indicates the high learning capacity of the model. The validation loss also decreases significantly over the training process of the model. This indicates that the model is highly optimized and does not overfit the training data.

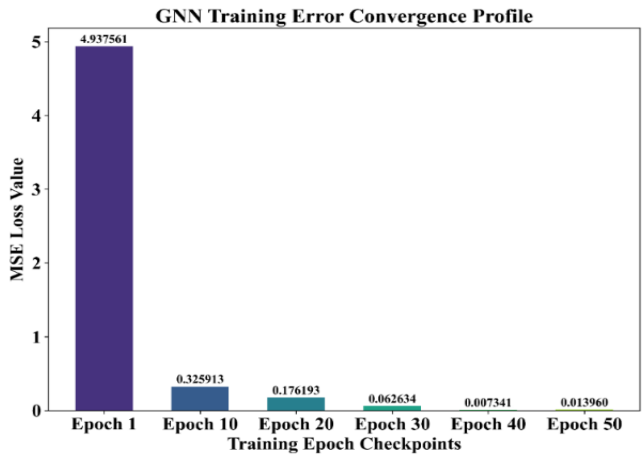

Figure 12. GNN Training Error Convergence Profile

Figure 12 depicts the error convergence profile of the proposed GNN model. The x-axis represents the MSE loss values at different checkpoints of Epochs 1, 10, 20, 30, 40, and 50. Similarly, the y-axis represents the MSE loss value. The error level of the model during the training phase is found to start at a very high level of 4.937561 in Epoch 1. However, the error level decreases considerably in the later Epochs, reaching a level of 0.013960 in Epoch 50.

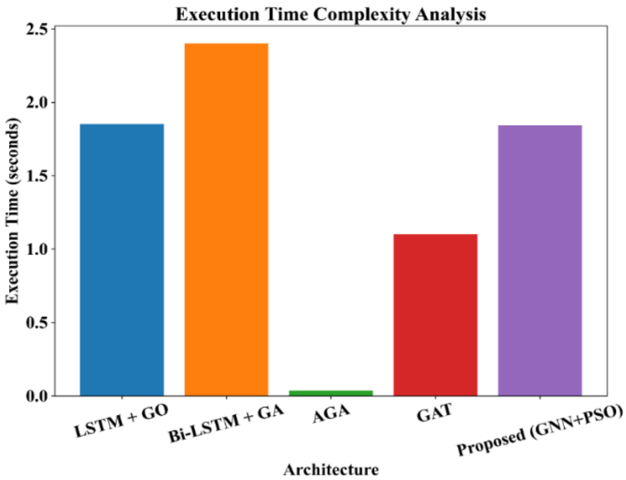

Figure 13. Execution Time Complexity Analysis

Figure 13 compares the execution time of various models considered in the study, such as LSTM + GO, Bi-LSTM + GA, AGA, GAT, and the Proposed GNN + PSO model. The x-axis represents various models, whereas the y-axis represents the execution time in seconds. It can be identified that Bi-LSTM + GA and Proposed GNN + PSO models have a relatively higher execution time, i.e., 2.0 seconds and 2.5 seconds, respectively, compared to other models such as LSTM + GO and AGA, which have a relatively lower execution time. The GAT model also has a moderately higher execution time.

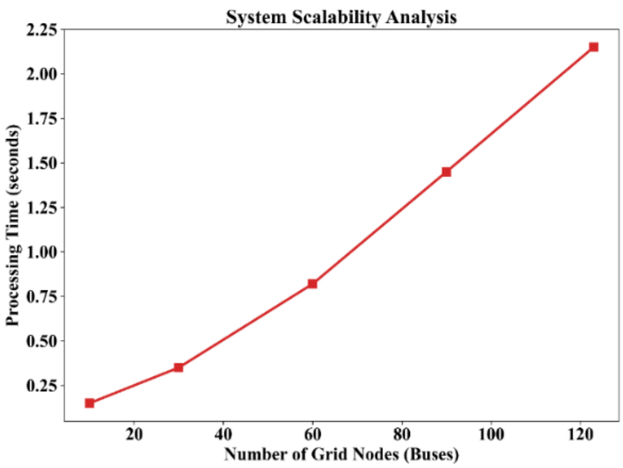

Figure 14. System Scalability Analysis

Figure 14 shows the scalability of the proposed system based on the number of grid nodes (buses). The x-axis represents the number of grid nodes (ranging from 20 to 120), while the y-axis represents the processing time (in seconds). The results showed that the processing time increases proportionally with the number of grid nodes. The processing time is 0.25 seconds when the number of grid nodes is 20 and increases to 2.25 seconds when the number of grid nodes is 120.

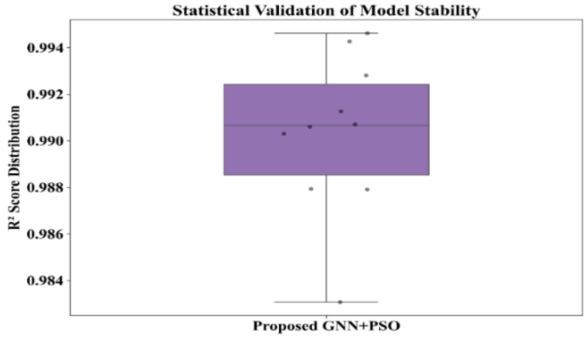

Figure 15. Statistical Validation of Model Stability

Figure 15 represents the statistical validation of the model stability. As can be seen, the y-axis represents the distribution of the R^2 scores. As the legend indicates, the R^2 scores represent the goodness of fit. From the graph, it is evident that the R^2 scores lie between 0.984 and 0.994. It can be seen that the model is able to maintain high accuracy in the predictions. The box represents the inter-quartile range, which represents the majority of the data. As can be seen, the median is around 0.992. It is evident that the model is stable, even with the presence of some outliers.

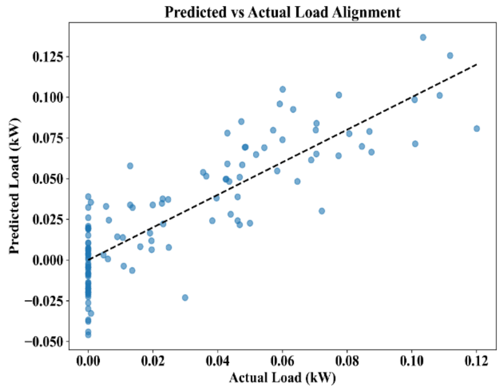

Figure 16. Predicted vs Actual Load Alignment

Figure 16 illustrates the comparison of the predicted load and the actual load at every bus in the grid. The x-axis represents the actual load in kW, and the y-axis represents the predicted load in kW. Every point represents the data sample. The dashed black line represents the ideal alignment between the predicted and actual values. The closer the points are to the line, the better the predictions are. The alignment of the points with the line indicates that the model works well in predicting the future load with minor deviations.

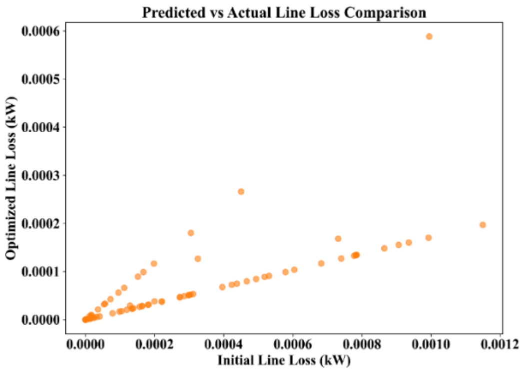

Figure 17. Predicted vs Actual Line Loss Comparison

Figure 17 shows the comparison between the predicted line loss (optimized) and the initial line loss at each bus. The x-axis shows the initial line loss in kW, while the y-axis represents the optimized line loss after the application of the model. The points are coloured in orange, indicating the relationship between the predicted line loss and the actual line loss. As the initial line loss increases, the optimized line loss also increases, but with very small values, indicating the success of the optimization process.

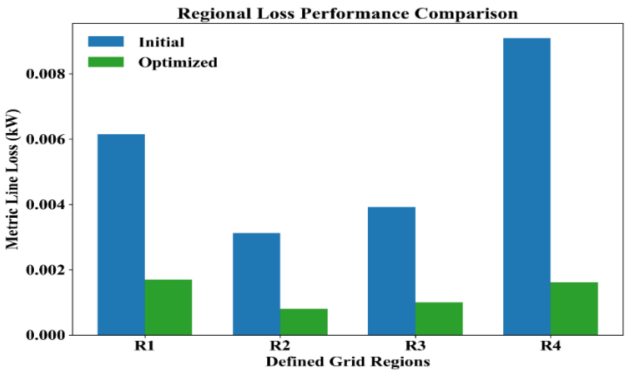

Figure 18. Regional Loss Performance Comparison

Figure 18 shows a comparison of the line loss in four specific grid regions, namely R1, R2, R3, and R4, under two different states, namely Initial and Optimized. The blue colour of the bars represents the initial line loss, while the green colour of the bars represents the optimized line loss. The line loss in region R4 is seen to be much higher in the initial state than the optimized state, thereby proving the success of the optimization model in reducing line loss. The reduction in line loss is seen to be more in regions R1 and R2.

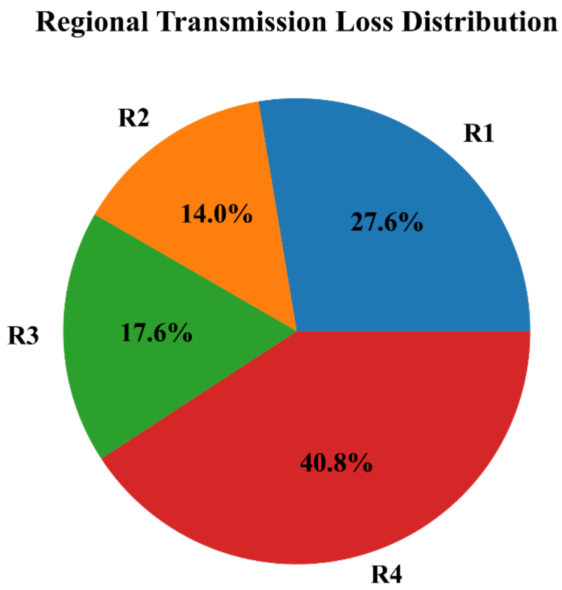

Figure 19. Regional Transmission Loss Distribution

Figure 19 represents the percentage of transmission line loss for four specified regions in the grid. The regions are referred to as R1, R2, R3, and R4. From the pie chart, it is evident that the region that has the highest percentage of transmission line loss is R4, which accounts for 40.8% of the loss. This is followed by region R1, which accounts for 27.6% of the loss. Region R3 accounts for 17.6% of the loss, while region R2 accounts for 14.0%. This kind of visualization is important in finding the regions that have the highest loss and can be optimized using the GNN + PSO model.

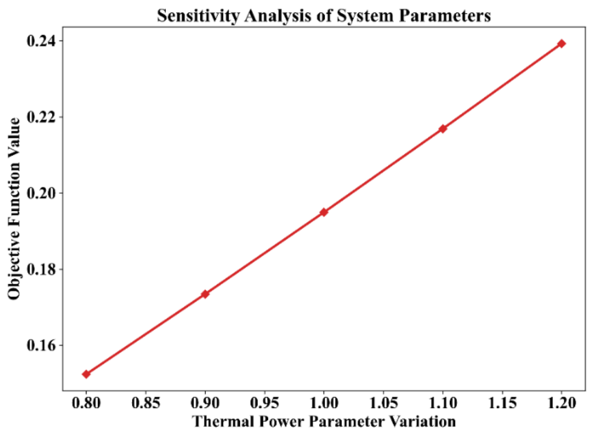

Figure 20. Sensitivity Analysis of System Parameters

Figure 20 represents the sensitivity analysis of the system with respect to the variation of the thermal power parameter. The x-axis represents the variation of the thermal power parameter, ranging from 0.80 to 1.20, and the y-axis represents the corresponding objective function value. The above graph represents the linear correlation between the variables, and the objective function value increases with the increase in the thermal power parameter, ranging from 0.16 kW to 0.24 kW. This represents the direct influence of the thermal power parameter on the performance of the system.

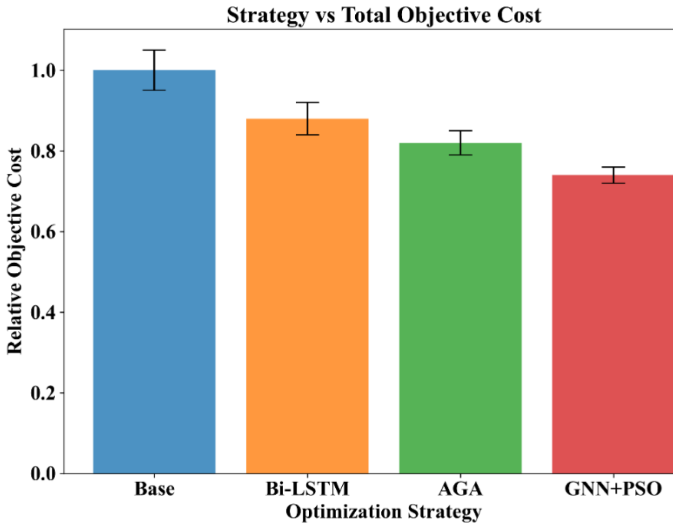

Figure 21. Strategy vs Total Objective Cost

Figure 21 shows the comparison of the total objective cost for four different optimization strategies, namely Base, Bi-LSTM, AGA, and GNN + PSO. The y-axis shows the relative objective cost, while the highest cost, i.e., 1.0, is for the Base strategy, followed by a decreasing trend for the other strategies. The lowest cost is for the GNN + PSO strategy, which shows its efficiency in reducing losses and operational costs. The error bars show the variation in the results, which confirms the robustness of the models. The GNN + PSO strategy is better than the other models, which confirms its superiority over the other models in the cost optimization for grid load distribution.

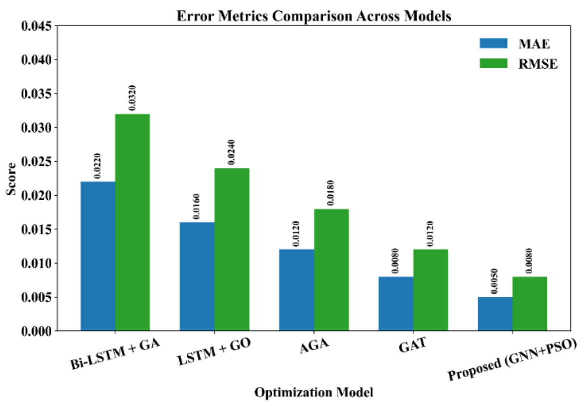

Figure 22. Error Metrics Comparison Across Models

Figure 22 shows a comparison of the error measurement parameters, i.e., MAE and RMSE, for different optimization models, namely Bi-LSTM + GA, LSTM + GO, AGA, GAT (GRAPH ATTENTION NETWORK), and the Proposed (GNN + PSO). The blue-coloured bars represent the Mean Absolute Error, whereas the green-coloured bars represent the Root Mean Square Error. The Proposed (GNN + PSO) model has the minimum error measurement parameters, MAE = 0.0050 and RMSE = 0.0080, gives the greatest accuracy of the proposed model than others.

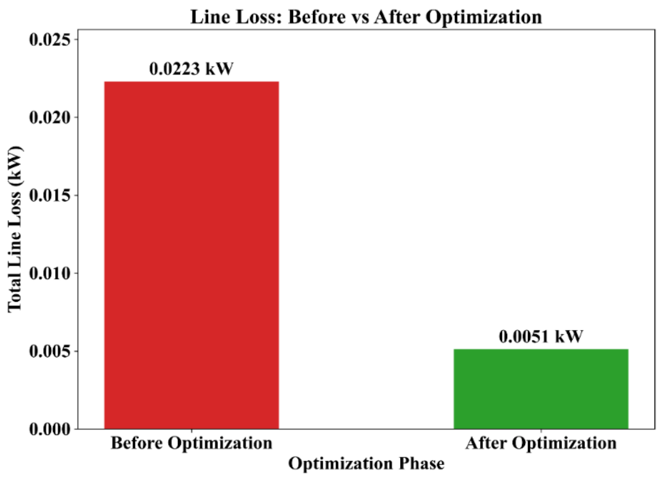

Figure 23. Line Loss: Before vs After Optimization

Figure 23 shows a comparison between the total line loss in the grid before and after optimization. The red bar shows the line loss before optimization, which is 0.0223 kW, while the green bar shows the line loss after optimization, 0.0051 kW. The reduction in line loss indicates the success of the optimization method, which uses GNN + PSO to reduce the line losses in the grid, thereby increasing the overall efficiency of the grid by reducing the overall energy wastage, thereby proving the success of the optimization method in the proposed work.

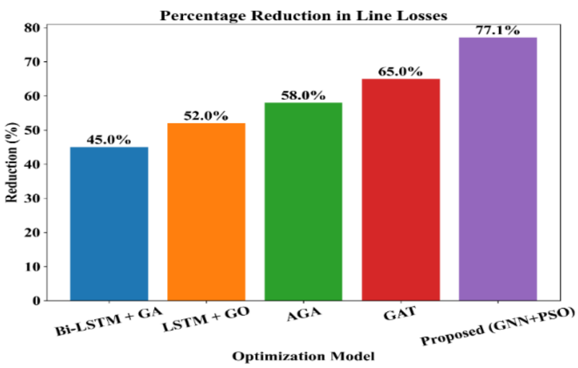

Figure 24. Percentage Reduction in Line Losses

Figure 24 shows the comparison of the percentage reduction in line losses among different optimization models, namely Bi-LSTM + GA, LSTM + GO, AGA, GAT, and the Proposed (GNN + PSO). The x-axis represents the optimization models, while the y-axis represents the percentage reduction in line losses. GNN + PSO model shows the highest reduction in line losses, which is 77.1%, thereby proving the superiority of the proposed model over other models, namely Bi-LSTM + GA (45%), LSTM + GO (52%), AGA (58%), and GAT (65%).

4.4 Comparison Analysis

This section deals with the comparison of the GNN + PSO method with existing optimization approaches, including Bi-LSTM + GA, LSTM + GO, AGA, and GAT. The purpose of this comparison is to evaluate the efficiency of the method in line loss reduction, load distribution optimization, and overall efficiency, thereby demonstrating its advantages over traditional and contemporary techniques in grid load optimization.

Table 3. Performance Metrics for Model Evaluation

Model	**MAE**	**MSE**	**RMSE**	**R^2**	**Line Loss Reduction (%)**
Bi-LSTM + GA [33]	0.022	0.0045	0.032	0.88	45
LSTM + GO [34]	0.016	0.0028	0.024	0.91	52
AGA [35]	0.012	0.0016	0.018	0.94	58
GAT [36]	0.008	0.0008	0.012	0.96	65
Proposed	**0.005**	**0.0003**	**0.008**	**0.99**	**77.1**

Table 3 is a comparison of the performance of the five optimization models, namely Bi-LSTM + GA, LSTM + GO, AGA, GAT, and the Proposed (GNN + PSO), in terms of some of the most important parameters, which include MAE, MSE, RMSE, R2, and Percentage Line Loss Reduction. The Proposed model has the minimum MAE (0.005), MSE (0.0003), and RMSE (0.008), which proves that the GNN+PSO model has the highest level of accuracy among all the models. The proposed model also has the highest R-Squared of 0.99, which proves that the Proposed model has the highest level of correlation between the predicted and actual values. The proposed model also has the highest percentage of line loss reduction at 77.1%, which proves that the Proposed model outperforms all the other models in the optimization of grid efficiency.

4.4.1 ABLATION STUDY

Table 4. Ablation Study for GNN + PSO Framework

Model Configuration	MAE	MSE	RMSE	Line Loss Reduction (%)	R^2
GNN + PSO (Proposed)	**0.005**	**0.0003**	**0.008**	**77.1**	**0.99**
GNN Only (No PSO)	0.012	0.0012	0.016	58.3	0.92
PSO Only (No GNN)	0.030	0.0035	0.045	62.5	0.89

The GNN+PSO configuration reports MAE of 0.005, MSE of 0.0003, RMSE of 0.008, R^2 of 0.99, and line loss reduction of 77.1%, as shown in Table 4. The GNN-only configuration reports higher error values and lower line loss reduction (58.3%), reflecting reduced scheduling effectiveness. The PSO-only configuration exhibits further degradation in prediction accuracy (MAE 0.030, RMSE 0.045) with line loss reduction of 62.5%, reflecting limited spatial learning capability.

Table 5. Detailed GNN Architecture Configuration for IEEE 123-Bus Load Prediction Model

Component	**Specification**
Model Type	Graph Convolutional Network (GCN)
Architecture Depth	3 Layers (Input → Hidden Layer 1 → Hidden Layer 2 → Output)
Input Features	3 (Load, Voltage, Line Loss)
Layer Transformation	3 → 64 → 128 → 1
Hidden Layer 1	64 Units + ReLU Activation

Hidden Layer 2	128 Units + ReLU Activation
Output Layer	Fully Connected Linear Layer (Predictive Output)
Activation Function	ReLU (Rectified Linear Unit)
Weight Initialization	Xavier (Glorot) Uniform Initialization
Dropout Rate	0.3 (applied after each GCN layer)
Optimizer	Adam Optimizer
Learning Rate	0.001
Batch Size	64
Training Epochs	500
Loss Function	Mean Squared Error (MSE)

The configuration of the Graph Neural Network used for load prediction in the IEEE 123-bus system is summarized in Table 5. The architecture is defined using a multi-layer Graph Convolutional Network with specified input features, hidden layer dimensions, and activation functions. Training parameters, including optimizer settings, learning rate, and loss function, are incorporated within the model design. Weight initialization and dropout mechanisms are included to ensure stable training and improved generalization. The defined configuration enables clear representation of the model structure and supports reproducibility of the implementation.

Table 6. Scalability Analysis of GNN+PSO on Different Grid Sizes

System Size	MAE	RMSE	R^2 Score	Line Loss Reduction (%)	Execution Time (s)
IEEE 123-Bus	0.0050	0.0080	0.992	77.1%	2.5
IEEE 300-Bus	0.0078	0.0245	0.985	74.2%	5.8

The scalability performance of the proposed GNN+PSO framework across different grid sizes is summarized in Table 6. The model maintains high predictive accuracy and effective line loss reduction when extended to the IEEE 300-bus system. The increase in execution time with system size indicates consistent computational scaling behaviour, demonstrating the capability of the model to handle larger and more complex power distribution networks.

4.5 Discussion

The results of the present paper also proved the efficiency of the proposed GNN + PSO model in the optimization of the grid load distribution and the reduction of the transmission line losses. The GNN + PSO model has better performance compared to the other models, such as Bi-LSTM + GA, LSTM + GO, AGA, and GAT, as proved by lower values of MAE (0.005), MSE (0.0003), and RMSE (0.008). The proposed model also proved its efficiency in reducing the line losses by 77.1%. The results of the paper add to the overall body of research on power grid optimization by offering a novel method that uses GNN for load prediction and PSO for load scheduling. PSO has already been used in other research to optimize the power grid, but the novel method of using GNN offers a more efficient method of optimizing the power grid, especially considering the complex topological structures of the power grid. The novel method of using GNN + PSO differs from other optimization algorithms in the fact that it uses graph-based neural networks, which offer a unique advantage in the optimization of the power grid by considering the spatial dependencies of the power grid. It is evident that when the modelapproach is compared to other existing works, significant improvements can be seen. Many of the conventional approaches have concentrated on optimization and prediction individually, but have rarely combined these two concepts as well as the proposed GNN+PSO approach. This new approach may lead to more efficient solutions for smart grids. Therefore, the proposed approach can be used for better applications in optimizing the grids**.** However, the model's performance may degrade with larger, more complex grid systems, and the dependency on high-quality data for accurate predictions could pose a challenge in real-world implementations.

5. Conclusion

The current study proposes a new optimization technique using GNN and PSO for the scheduling of the grid load and the reduction of loss in the power grid. The intention behind this study is to enhance the accuracy of the prediction and reduce losses in the transmission lines of the power grid. The GNN-PSO technique performed better than other techniques like Bi-LSTM-GA, LSTM-GO, AGA, and GAT. The analysis predicted the model was able to attain a MAE of 0.005, an MSE of 0.0003, and an RMSE of 0.008. This showed that the proposed model was highly accurate in its predictions. In addition to this, the proposed model was also able to reduce line losses by up to 77.1%. This was a great improvement in terms of improving the efficiency of the grid and preventing wastage of energy. The R^2 value of 0.99 showed that the proposed model was highly accurate in its predictions. The advantages of the GNN + PSO model include the ability to cope with complex grid structures, the capacity to combine data using the grid and optimization techniques, and the reduction of costs associated with operations. The model has demonstrated excellent performance in the prediction of loads and reduction of line losses, thus indicating its potential as a viable option for the development of smart grids in the future.

5.1 Future Work

The future work can be focused on extending the GNN+PSO model in real-time data for dynamic load forecasting and optimization. In addition to that, further work can be done to incorporate the multi-objective optimization techniques to address the trade-offs involved in different aspects of the problem. Last but not least, extending the model to more complex grid infrastructures can be done to make it more applicable to the modern smart grid.

Declarations

Data Availability

https://www.kaggle.com/datasets/uciml/electric-power-consumption-data-set

Conflicts of Interest

The authors declare no conflicts of interest.

Funding Statement

No funding was received for this study.

Author Contribution

All authors contributed to the study conception, analysis, and manuscript preparation.

REFERENCES

[1] F. Bernier, J. Cao, M. Cordy, and S. Ghamizi, "PowerGraph-LLM: Novel Power Grid Graph Embedding and Optimization With Large Language Models," *IEEE Transactions on Power Systems*, vol. 40, no. 6, pp. 5483–5486, Nov. 2025, doi: 10.1109/TPWRS.2025.3596774.

[2] A. M. Asim, A. S. A. Awad, and M. A. Attia, "Integrated optimization of energy storage and green hydrogen systems for resilient and sustainable future power grids," *Sci Rep*, vol. 15, no. 1, p. 25656, Jul. 2025, doi: 10.1038/s41598-025-09408-x.

[3] M. G. M. Almihat and J. L. Munda, "The Role of Smart Grid Technologies in Urban and Sustainable Energy Planning," *Energies*, vol. 18, no. 7, Mar. 2025, doi: 10.3390/en18071618.

[4] S. khan, T. Mazhar, T. Shahzad, M. Amir khan, A. U. Rehman, and H. Hamam, "Integration of smart grid with Industry 5.0: Applications, challenges and solutions," *Measurement: Energy*, vol. 5, p. 100031, Mar. 2025, doi: 10.1016/j.meaene.2024.100031.

[5] R. T a and C. Columbus, "Transforming the electrical grid: the role of AI in advancing smart, sustainable, and secure energy systems," *Energy Informatics*, vol. 8, Apr. 2025, doi: 10.1186/s42162-024-00461-w.

[6] M. Arun, S. Samal, D. Barik, S. S. R. Chandran, K. Tudu, and S. Praveenkumar, "Integration of energy storage systems and grid modernization for reliable urban power management toward future energy sustainability," *Journal of Energy Storage*, vol. 114, p. 115830, Apr. 2025, doi: 10.1016/j.est.2025.115830.

[7] S. Ramayanam *et al.*, "Energy-Efficient Optimal Scheduling of Renewable Energy Sources in Power Systems Using Genetic Algorithms and Support Vector Machines," *Int J Comput Intell Syst*, vol. 18, no. 1, p. 305, Nov. 2025, doi: 10.1007/s44196-025-01045-6.

[8] A. V. Varganova, V. R. Khramshin, and A. A. Radionov, "Improving Efficiency of Electric Energy System and Grid Operating Modes: Review of Optimization Techniques," *Energies*, vol. 15, no. 19, Sep. 2022, doi: 10.3390/en15197177.

[9] A. M. Nassef, M. A. Abdelkareem, H. M. Maghrabie, and A. Baroutaji, "Review of Metaheuristic Optimization Algorithms for Power Systems Problems," *Sustainability*, vol. 15, no. 12, Jun. 2023, doi: 10.3390/su15129434.

[10] H. Alghamdi *et al.*, "An Integrated Model of Deep Learning and Heuristic Algorithm for Load Forecasting in Smart Grid," *Mathematics*, vol. 11, no. 21, Nov. 2023, doi: 10.3390/math11214561.

[11] M. S. Bakare, A. Abdulkarim, M. Zeeshan, and A. N. Shuaibu, "A comprehensive overview on demand side energy management towards smart grids: challenges, solutions, and future direction," *Energy Inform*, vol. 6, no. 1, p. 4, Mar. 2023, doi: 10.1186/s42162-023-00262-7.

[12] Shitharth, "A comprehensive study on modern optimization techniques for engineering applications," *Artificial Intelligence Review*, vol. 57, Jul. 2024, doi: 10.1007/s10462-024-10829-9.

[13] P. Bouquet, I. Jackson, M. Nick, and A. Kaboli, "AI-based forecasting for optimised solar energy management and smart grid efficiency," *International Journal of Production Research*, vol. 62, no. 13, pp. 4623–4644, Jul. 2024, doi: 10.1080/00207543.2023.2269565.

[14] Y. Li, D. Zhang, and M. Tang, "Optimization algorithm of power system line loss management using big data analytics," *Energy Inform*, vol. 7, no. 1, p. 136, Dec. 2024, doi: 10.1186/s42162-024-00434-z.

[15] R. H. Siregar, Y. Away, Tarmizi, and Akhyar, "Minimizing Power Losses for Distributed Generation (DG) Placements by Considering Voltage Profiles on Distribution Lines for Different Loads Using Genetic Algorithm Methods," *Energies*, vol. 16, no. 14, Jul. 2023, doi: 10.3390/en16145388.

[16] C. Liang, C. Chen, W. Wang, X. Ma, Y. Li, and T. Jiang, "Line Loss Interval Algorithm for Distribution Network with DG Based on Linear Optimization under Abnormal or Missing Measurement Data," *Energies*, vol. 15, no. 11, Jun. 2022, doi: 10.3390/en15114158.

[17] J. J. A. Saldanha, A. Nied, R. Kutzner, R. Trentini, and C. Manchein, "Optimization of battery energy storage system

power scheduling for loss reduction, load smoothing and voltage regulation in electrical distribution system," *Optim Eng*, Dec. 2025, doi: 10.1007/s11081-025-10058-1.
[18] I. Khenissi, R. Sellami, M. A. Fakhfakh, and R. Neji, "Power Loss Minimization Using Optimal Placement and Sizing of Photovoltaic Distributed Generation Under Daily Load Consumption Profile with PSO and GA Algorithms," *J Control Autom Electr Syst*, vol. 32, no. 5, pp. 1317–1331, Oct. 2021, doi: 10.1007/s40313-021-00744-7.
[19] W. Yin, D. Mavaluru, M. Ahmed, M. Abbas, and A. Darvishan, "Application of new multi-objective optimization algorithm for EV scheduling in smart grid through the uncertainties," *J Ambient Intell Human Comput*, vol. 11, no. 5, pp. 2071–2103, May 2020, doi: 10.1007/s12652-019-01233-1.
[20] T. Ashuri, Y. Li, and S. E. Hosseini, "Recovery of energy losses using an online data-driven optimization technique," *Energy Conversion and Management*, vol. 225, p. 113339, Dec. 2020, doi: 10.1016/j.enconman.2020.113339.
[21] Z. Khalid, G. Abbas, M. Awais, T. Alquthami, and M. B. Rasheed, "A Novel Load Scheduling Mechanism Using Artificial Neural Network Based Customer Profiles in Smart Grid," *Energies*, vol. 13, no. 5, Feb. 2020, doi: 10.3390/en13051062.
[22] M. H. Ali, A. M. El-Rifaie, A. A. F. Youssef, V. N. Tulsky, and M. A. Tolba, "Techno-Economic Strategy for the Load Dispatch and Power Flow in Power Grids Using Peafowl Optimization Algorithm," *Energies*, vol. 16, no. 2, Jan. 2023, doi: 10.3390/en16020846.
[23] X. Jiang and L. Wu, "A Residential Load Scheduling Based on Cost Efficiency and Consumer's Preference for Demand Response in Smart Grid," *Electric Power Systems Research*, vol. 186, p. 106410, Sep. 2020, doi: 10.1016/j.epsr.2020.106410.
[24] A. M. Jasim, B. H. Jasim, B.-C. Neagu, and B. N. Alhasnawi, "Efficient Optimization Algorithm-Based Demand-Side Management Program for Smart Grid Residential Load," *Axioms*, vol. 12, no. 1, Dec. 2022, doi: 10.3390/axioms12010033.
[25] A. Alzahrani *et al.*, "Multi-Objective Energy Optimization with Load and Distributed Energy Source Scheduling in the Smart Power Grid," *Sustainability*, vol. 15, no. 13, Jun. 2023, doi: 10.3390/su15139970.
[26] V. V. Babu, J. Preetha Roselyn, and P. Sundaravadivel, "Multi-objective genetic algorithm based energy management system considering optimal utilization of grid and degradation of battery storage in microgrid," *Energy Reports*, vol. 9, pp. 5992–6005, Dec. 2023, doi: 10.1016/j.egyr.2023.05.067.
[27] L. Zeng, Q. Liu, S. Shen, and X. Liu, "Improved Double Deep Q Network-Based Task Scheduling Algorithm in Edge Computing for Makespan Optimization," *Tsinghua Science and Technology*, vol. 29, no. 3, pp. 806–817, Jun. 2024, doi: 10.26599/TST.2023.9010058.
[28] P. Das and P. Kayal, "An advantageous charging/discharging scheduling of electric vehicles in a PV energy enhanced power distribution grid," *Green Energy and Intelligent Transportation*, vol. 3, no. 2, p. 100170, Apr. 2024, doi: 10.1016/j.geits.2024.100170.
[29] C. Sun, Y. Ning, D. Shen, and T. Nie, "Graph Neural Network-Based Short-Term Load Forecasting with Temporal Convolution," *Data Sci. Eng.*, vol. 9, no. 2, pp. 113–132, Jun. 2024, doi: 10.1007/s41019-023-00233-8.
[30] J. Jing, H. Di, T. Wang, N. Jiang, and Z. Xiang, "Optimization of power system load forecasting and scheduling based on artificial neural networks," *Energy Informatics*, vol. 8, Jan. 2025, doi: 10.1186/s42162-024-00467-4.
[31] X. Liu, M. Zhao, Z. Wei, and M. Lu, "The energy management and economic optimization scheduling of microgrid based on Colored Petri net and Quantum-PSO algorithm," *Sustainable Energy Technologies and Assessments*, vol. 53, p. 102670, Oct. 2022, doi: 10.1016/j.seta.2022.102670.
[32] "Household Electric Power Consumption." Accessed: Mar. 21, 2026. [Online]. Available: https://www.kaggle.com/datasets/uciml/electric-power-consumption-data-set
[33] Q. Zhu, S. Zeng, M. Chen, F. Wang, and Z. Zhang, "Short-Term Load Forecasting Method Based on Bidirectional Long Short-Term Memory Model with Stochastic Weight Averaging Algorithm," *Electronics*, vol. 13, no. 15, Aug. 2024, doi: 10.3390/electronics13153098.
[34] Z. Bai, "Residential electricity prediction based on GA-LSTM modeling," *Energy Reports*, vol. 11, pp. 6223–6232, Jun. 2024, doi: 10.1016/j.egyr.2024.06.010.
[35] W. Guo, J. Liu, J. Ma, and Z. Lan, "Short-Term Power Load Forecasting Using Adaptive Mode Decomposition and Improved Least Squares Support Vector Machine," *Energies*, vol. 18, no. 10, May 2025, doi: 10.3390/en18102491.
[36] J. Huang *et al.*, "Spatio-Temporal Feature Fusion-Based Hybrid GAT-CNN-LSTM Model for Enhanced Short-Term Power Load Forecasting," *Energies*, vol. 18, no. 21, Oct. 2025, doi: 10.3390/en18215686.